

Title: Supercritical CO₂ assisted synthesis and concentration of monoacylglycerides rich in omega-3 polyunsaturated fatty acids

Authors

Rodrigo Melgosa* (rmgomez@ubu.es)

María Teresa Sanz (tersanz@ubu.es)

Óscar Benito-Román (obenito@ubu.es)

Alba Esther Illera (aeillera@ubu.es)

Sagrario Beltrán (beltran@ubu.es)

Address

Department of Biotechnology and Food Science (Chemical Engineering Division)

University of Burgos, Plaza Misael Bañuelos s/n, 09001 Burgos, Spain

Declarations of interest: none

* Corresponding author. Tel.: +34-947258810; Fax: +34-947258831; e-mail: rmgomez@ubu.es

Abstract

Supercritical carbon dioxide (SC-CO₂) has been used as solvent in the ethanolysis of fish oil rich with omega-3 polyunsaturated fatty acids (n-3 PUFAs) by Lipozyme 435. The effect of experimental conditions: initial ethanol-to-oil molar ratio (MR, 6:1-76:1), pressure (10-30 MPa), and temperature (323-343 K) on the reaction performance has been studied. Experimental results have been fitted to a kinetic model based on a Ping Pong Bi Bi mechanism. High accumulation of monoacylglycerides (MAGs) has been observed in short reaction times (90 min at MR = 76:1, 10 MPa, 323 K). Subsequent purification of reaction products by supercritical fluid extraction (SFE) in the experimental range 10-28 MPa and 298-333 K yielded an extract rich with fatty acid ethyl esters (FAEE) (up to 99.46 %wt.), and a raffinate with up to 82.25 %wt. MAG and 49.5 %wt. n-3 PUFAs.

Keywords

Omega 3; lipase; ethanolysis; supercritical carbon dioxide; supercritical fluid extraction

1. Introduction

Long-chain omega-3 polyunsaturated fatty acids (n-3 PUFAs), especially eicosapentaenoic (EPA, 20:5 n-3) and docosahexaenoic (DHA 22:6 n-3) acids, are essential nutrients with an important role in pre-natal, infant, child and adolescent development [1]. Furthermore, an adequate intake of n-3 PUFAs is related to a reduced risk of developing cardiovascular diseases [2], inflammatory conditions [3], and mental illnesses such as depression, Alzheimer's disease, and dementia [4–6].

Fish oil, as the fatty liquid obtained from fish rich in n-3 PUFAs, has attracted the interest of pharmaceutical and food industries since it constitutes a good source of these bioactive compounds. However, the EPA plus DHA content in fish oil is usually around 30 % wt. [7], so concentration and

formulation steps are needed in order to obtain nutraceuticals and food supplements with acceptable purity [8].

The production of n-3 PUFA concentrates usually involves a previous transesterification of the fish oil triacylglycerides (TAG) with a food-grade alcohol such as ethanol (EtOH), obtaining fatty acid ethyl esters (FAEE) and glycerol (GLY) as final products of the reaction. Reaction intermediaries, diacylglycerides and monoacylglycerides (DAG and MAG, respectively), can accumulate under certain conditions (e.g.: enzyme specificity) [9]. DAG and MAG are of particular interest since they have been widely used as emulsifying agents in the food and cosmetics industries. Moreover, novel nutraceutical products are also based on DAG and MAG, since they are reported to potentially prevent obesity and provide benefits in the treatment of chronic diseases such as diabetes and atherosclerosis [9]. Besides, several studies point to the MAG form as more bioavailable than FAEE, since the former are naturally absorbed by the enterocytes [10]. Subsequently, n-3 PUFAs need to be separated from the other fatty acids and reactants present in the reaction mixture. Different methods such as molecular distillation, low-temperature crystallization, urea complexation, or supercritical fluid fractionation can be used at industrial scale to obtain up to 90-95 % wt. n-3 PUFAs in FAEE form [11].

Traditional transesterification methods generally make use of acid or alkaline catalysts, which can lead to low selectivity and undesirable side reactions. Moreover, high temperatures involved in this process may cause oxidative deterioration of the fish oil. As an alternative, enzymatic transesterification of oils rich in n-3 PUFAs in supercritical fluids (SCFs) has been proposed for obtaining less oxidized n-3 PUFA concentrates, compared to conventional methods [12–14].

Supercritical carbon dioxide (SC-CO₂) is possibly the most used SCF due to the advantages provided at substituting organic solvents. CO₂ is non-toxic, non-flammable, and readily available at high

purity and low cost. The transport properties of SC-CO₂, including viscosity and diffusivity, are intermediate between those of gases and liquids, which greatly reduce mass transport limitations for reactions conducted in this media. In addition, CO₂ critical conditions are relatively mild, which allows operation with thermosensitive compounds such as n-3 PUFAs, and since it is a gas at atmospheric conditions, it is completely released from the reaction products by simple depressurization [15–17]. Besides, SC-CO₂ can be used not only as reaction media but also in the separation step, since the density-dependent solvent power of SC-CO₂ can be tailored through pressure and temperature variations in order to selectively extract different lipid compounds. In this sense, lipase-catalysed reactions in SC-CO₂ followed by supercritical fluid extraction (SFE) of the reaction products raises as a promising method for the purification of n-3 PUFAs [18,19].

Some studies on enzymatic ethanolysis of triacylglycerides in SC-CO₂ can be found in the literature, using different immobilized lipases from *Candida antarctica* (Lipozyme 435, Novozyme 435) [20–22], *Thermomucres lanuginosa* (Lipozyme TL IM) [23,24], and *Rhizomucor miehei* (Lipozyme RM IM) [21,25]. These studies are usually focused on the effect of enzyme loading, pressure, temperature, and initial molar ratio of substrates (MR) on the reaction performance. In a previous work [14], ethanolysis of fish oil in SC-CO₂ by Lipozyme RM IM (5 %wt. of substrates) was studied in the experimental range 7.5-30 MPa, 323-353 K, and MR = 2:1-38:1. Kinetic data were correlated using a semi-empirical model based on the mass balances of all the species in the reaction system. FAEE yields up to 86 %, and less oxidized reaction products compared to *tert*-pentanol and solvent-free media were obtained. However, low quantities of MAG were produced, which was possibly due to enhanced acyl-migration.

Several authors have stressed the importance of phase behavior in heterogeneous catalysis in SC-CO₂, since it allows control of selectivity and reaction rates due to its effect on the relative concentration of the reactants and their intimate contact [26,27]. However, the previously mentioned

studies do not report relative concentrations of reactants and solvent in the high-pressure reactor, and phase behavior of the reaction system is scarcely mentioned. This limitation is possibly linked to the low amount of experimental phase equilibria data available in the literature [27]. To cope with this issue, experimental phase equilibria data of the pseudo-ternary system SC-CO₂ (1) + ethanol (2) + fish oil (3) in the range 10-30 MPa and 323-343 K has been studied in a previous work [28]. Based on these data, we have been able to study the effect of initial phase behavior on the reaction performance and selectivity to MAG.

Application of liquid and supercritical CO₂ to separate MAG and fatty acid esters has been previously studied in the literature. Compton et al. [18] used liquid CO₂ (8.62 MPa, 298 K) to extract 2-MAG from the reaction products obtained after ethanolysis of triolein, achieving ~80 % yield relative to initial TAG, and reduced acyl-migration. More recently, Soto et al. [19] simulated a counter-current liquid and SC-CO₂ extraction process to refine MAG from a 80/20 (% wt.) mixture of fatty acid methyl esters (FAMES) and MAG, finding this process technically feasible to concentrate MAG up to 99.8 % wt purity.

In the present work, Lipozyme 435 from *Candida antarctica*, has been used in the ethanolysis of fish oil in SC-CO₂. This lipase is generally considered as non-specific, although it has been reported to behave as sn-1,3-specific when a high concentration of alcohol is present in the media [29]. The effect of phase behavior (expanded liquid or homogeneous system), ethanol concentration, and operating pressure and temperature on the reaction performance and selectivity to MAG have been assessed. Experimental kinetic data have been successfully explained by a kinetic model based on the Ping Pong Bi Bi mechanism. Additionally, SFE of the reaction products using liquid and SC-CO₂ as solvent has been performed at different pressure and temperature conditions, with the aim of selectively extract FAEE and concentrate MAG and n-3 PUFAs in the raffinate.

2. Experimental

2.1. Materials

Lipozyme 435, a lipase from *Candida antarctica* immobilized on a macroporous acrylic resin (Lewatit VP OC 1600), was purchased from Novozymes A/S (Denmark). Refined fish oil was provided by AFAMSA S.A. (Spain) being a mixture of tuna (*Thunnus* sp.) and sardine (*Sardina pilchardus*) oil. Fatty acid profile of the fish oil has been previously reported with 21.0 %wt. palmitic acid, 18.4 %wt. oleic acid, 24.9 %wt. DHA, and 6.9 %wt. EPA [30]. According to this fatty acid composition, molecular weight of fish oil was estimated in 902 g/mol. Absolute ethanol (99.9 %) was purchased from Merck KGaA. Carbon dioxide (99.9%) was supplied by Air Liquide S.A. (Spain). All other chemicals used in different analyses were of analytical or HPLC grade.

2.2. Methods

2.2.1. Ethanolysis of fish oil in SC-CO₂

The ethanolysis reaction was performed in a high-pressure batch stirred tank reactor (HP-BSTR) made of stainless steel (SS-316) and having an internal volume of 100 mL. A scheme of the apparatus is given in Fig. 1. More details of the configuration of the HP-BSTR and the experimental procedure have been reported in a previous work [14].

Typically, known amounts of fish oil and ethanol were firstly tempered and added into the reactor. Initial loading was in the range 40-60 g, and ethanol:fish oil proportion according to the established initial molar ratio of substrates (MR). Subsequently, a certain amount of enzyme (10% wt. of substrates) was added and the reactor closed, connected to the pressure circuit and placed in a thermostatic water bath. Afterwards, a known quantity of pressurized CO₂ was fed into the reactor by means of a high-pressure syringe pump (ISCO 260 D). Once the desired pressure and temperature were reached, magnetic stirring was connected and the reaction was initiated. During the experiment, pressure and temperature were controlled by means of a pressure transducer with an uncertainty of ± 0.05 MPa, and an immersed thermocouple (uncertainty ± 0.1 K), respectively. Samples from the

bottom of the reactor were taken periodically and collected in glass screw-top vials, which were stored at $-18\text{ }^{\circ}\text{C}$ prior to analysis. Pressure drops up to 0.5 MPa were observed during the withdrawal of the samples, which were compensated by feeding fresh SC-CO₂ into the reactor. According to the low mass of the samples (ca. 0.1 g) compared with the initial loading of the HP-BSTR, disturbances of the batch process were considered negligible.

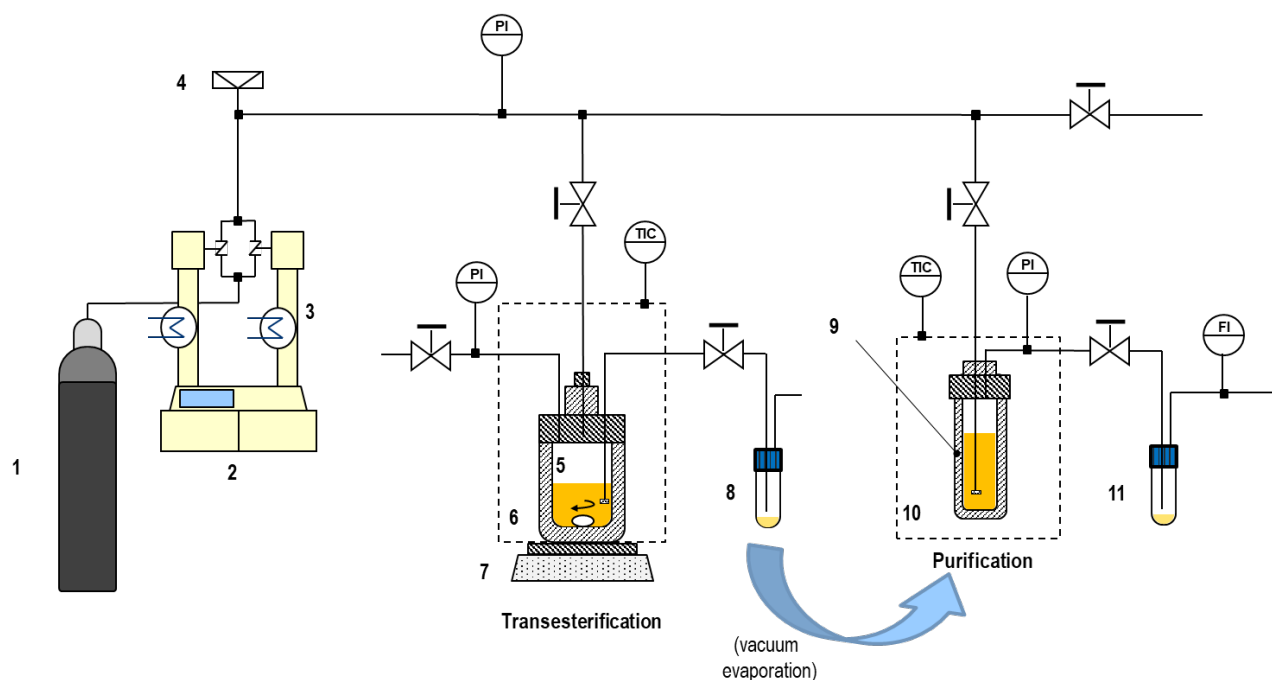


Figure 1. Experimental set-up for lipase-catalysed ethanolsis of fish oil and purification of reaction products using SC-CO₂. 1: CO₂ cylinder; 2: syringe pump; 3: cryostat; 4: rupture disk; 5: high-pressure batch stirred tank reactor; 6: thermostatic water bath; 7: magnetic stirrer; 8: sampling device; 9: high-pressure extractor; 10: thermostatic oven; 11: separator.

Based on previous studies [14,31], experimental conditions were varied from 10 to 30 MPa, 323 to 343 K, and MR from 6:1 to 76:1 (Table 1). Taking into account the initial loading of the reactor and experimental phase equilibria data of the pseudoternary system CO₂ (1) + ethanol (2) + fish oil (3) [28], the reaction is expected to take place in an expanded liquid (exps. 1 and 4), or in a homogeneous system (exps. 2, 3, 5, and 6). Reaction experiments have been carried out in duplicate.

Table 1. Experimental conditions for the ethanolysis of fish oil catalysed by Lipozyme 435 in SC-CO₂ and HP-BSTR loading of CO₂ (1), ethanol (2) and fish oil (3) (mass fraction) for each run.

run	p (MPa)	T (K)	MR (ethanol:oil)	Initial composition		
				w ₁	w ₂	w ₃
1	10	323	6:1	0.4455	0.1295	0.4250
2	10	323	6:1	0.1756	0.1943	0.6301
3	10	323	76:1	0.4139	0.4567	0.1294
4	10	343	76:1	0.3774	0.4948	0.1278
5	30	323	76:1	0.5110	0.3885	0.1005
6	30	343	76:1	0.4322	0.4499	0.1179

Standard uncertainties: $u(p) = \pm 0.5$ MPa, $u(T) = \pm 0.1$ K, $u(w_i) = \pm 0.005$.

2.2.2. Chromatographic analyses

Neutral lipid profile of the reaction samples was determined by normal phase high-performance liquid chromatography (NP-HPLC), quantifying total amounts of FAEE, DAG, MAG, and unreacted TAG. Free fatty acids (FFA) were not detected ($< 0.1\%$ wt.). Chromatographic equipment, method and calibration procedure have been described elsewhere [32].

GLY content was measured by means of High-Temperature Gas Chromatography (HT-GC). Chromatographic equipment, method and calibration procedure have been previously described [31].

Unreacted ethanol (n_{EtOH} , mmol) was theoretically calculated considering the reaction stoichiometry, in which the production of 1 mol of FAEE consumes 1 mol of EtOH, giving:

$$n_{\text{EtOH}} = n_{\text{EtOH}}^0 - n_{\text{FAEE}} \quad (1)$$

where n_{EtOH}^0 is the initial loading of ethanol (mmol).

Fatty acid profile analysis was performed by GC, following the AOAC official method [33]. The analysis was performed in a Hewlett Packard 6890 N GC system equipped with an auto-sampler (7683B series) and a flame ionization detector (FID). The column used was a fused silica capillary column (OmegawaxTM-320, 30 m \times 0.32 mm i.d.). Helium (1.8 ml·min⁻¹) was used as a carrier gas.

All compositions reported in this work represent the average of at least three independent measurements.

2.2.3. Purification of reaction products

The reaction products obtained after ethanolysis of fish oil in SC-CO₂ were subjected to SFE at different conditions in order to concentrate their major components, MAG in the raffinate and FAEE in the extract. The global scheme of the experimental set-up is depicted in Fig. 1.

Firstly, the collected reaction products were submitted to vacuum evaporation (Heidolph) at 303 K and 70 mbar to eliminate most of the unreacted EtOH. Immediately afterwards, a known amount (7.0 g) of the non-volatile residue was mixed with an equal amount of glass beads ($\varnothing = 3$ mm,) and introduced into a 30 mL laboratory-scale SFE vessel (Fig. 1, right). Free volume in the extraction system (extractor volume minus volume of glass beads) was approximately 25 mL. Subsequently, the extractor was placed in an oven in order to control temperature, which was varied between 298 and 333 K. Once the system was pre-heated, CO₂ was charged into the extraction vessel up to the desired pressure (10-30 MPa) by means of a double-syringe high pressure pump (ISCO 260 D). When operating pressure was reached, the outlet valve was open and the flowing CO₂ with the dissolved ethanol and lipid derivatives was depressurized to atmospheric conditions, collecting the extract into an ice-cooled trap. At the same time, fresh CO₂ was fed continuously to the extractor through a capillary ended in a sintered-steel plate that improved the contact between feed and solvent. CO₂ mass flow was fixed at 1.8 ± 0.2 g/min, calculated taking into account the displacement of the pump syringes and the pressure and temperature conditions inside the pump cylinders. A low CO₂ mass flow was chosen in order to operate with low CO₂-to-feed mass ratios, which enhances the selectivity of the SFE process [19].

SFE was performed during 30 min. After that, the system was depressurized and the extract and raffinate fractions were collected and weighed in order to calculate the extraction yield ($\epsilon_{\text{extract}}$) and the raffinate yield ($\epsilon_{\text{raffinate}}$), which are defined as:

$$\epsilon_{\text{extract}} (\%) = \frac{\text{extract (g)}}{\text{feed (g)}} \cdot 100 \quad (2)$$

$$\varepsilon_{\text{raffinate}} (\%) = \frac{\text{raffinate (g)}}{\text{feed (g)}} \cdot 100 \quad (3)$$

The composition of the initial feed, extract, and raffinate was determined by NP-HPLC analysis, following the method described in section 2.2.2. Ethanol concentration was calculated by mass difference.

The recovery percentages for FAEE and MAG were calculated based on the total amount recovered in the extract and raffinate, respectively, and related to the initial amount of each compound present in the feed:

$$\text{FAEE Recovery} (\%) = \frac{\text{extract} \cdot \text{FAEE}_{\text{extract}}}{\text{feed} \cdot \text{FAEE}_{\text{feed}}} \cdot 100 \quad (4)$$

$$\text{MAG Recovery} (\%) = \frac{\text{raffinate} \cdot \text{MAG}_{\text{raffinate}}}{\text{feed} \cdot \text{MAG}_{\text{feed}}} \cdot 100 \quad (5)$$

In a SFE process, solubility differences between components of the feed mixture in CO₂-phase can be reflected in the values of the partition ratio or distribution constant ($K_{Di} = y_i/x_i$) [34]. In this work, empirical K -ratios for the main components FAEE and MAG were calculated in a similar way, taking into account the final concentrations of these species in the extract and raffinate.

$$K\text{-ratio}_{\text{FAEE}} = \frac{\text{FAEE}_{\text{extract}}}{\text{FAEE}_{\text{raffinate}}} \quad (6)$$

$$K\text{-ratio}_{\text{MAG}} = \frac{\text{MAG}_{\text{extract}}}{\text{MAG}_{\text{raffinate}}} \quad (7)$$

If $K\text{-ratio}_i$ is greater than unity, compound i will be preferentially extracted by SC-CO₂, and concentrated in the extract. If $K\text{-ratio}_i < 1$, then compound i will be recovered in the raffinate. Therefore, this value may serve as an indication of the solubility differences of FAEE and MAG in liquid and SC-CO₂.

2.3. Kinetic model for the ethanolysis reaction

The proposed mechanism for the lipase-catalysed ethanolysis of fish oil was formulated on the basis of the following assumptions:

- (1) Each ethanolysis reaction proceeds via a Ping Pong Bi Bi mechanism, assuming that transesterification takes place by (a) formation of the enzyme-substrate complex (E·T, E·D, and E·M), (b) release of the corresponding glyceride (DAG, MAG or GLY), leaving an acyl-enzyme intermediate (F), and (c) decomplexation of F after reaction with ethanol (EtOH), rendering a fatty acid ethyl ester (FAEE) and regenerating the enzyme (E) [35].
- (2) Water and FFA were not considered in the model, since they were not analytically detected in any reaction sample.
- (3) The inhibition by ethanol follows the competitive inhibition mechanism [35], forming an inhibited enzyme-ethanol complex (I).

A conceptual scheme of the reaction is shown in Fig. 2.

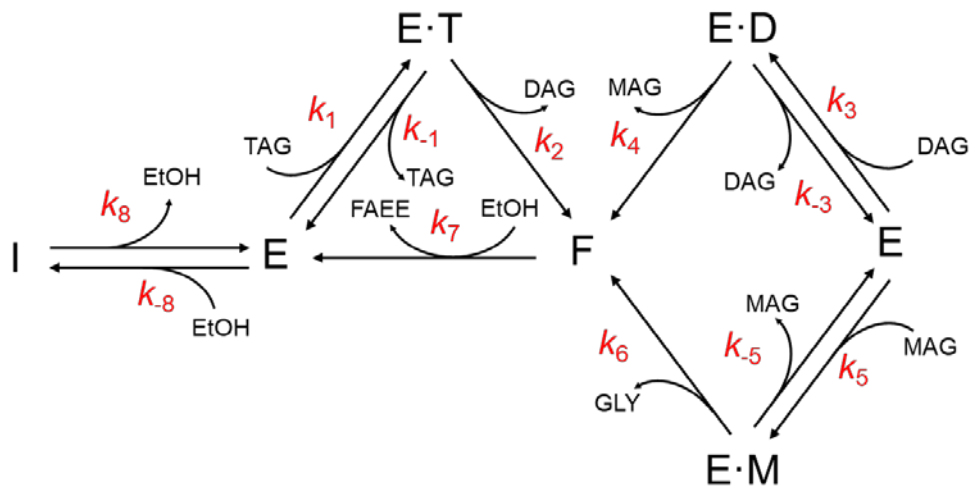


Figure 2. Schematic diagram of Ping Pong Bi Bi mechanism for ethanolysis of fish oil. TAG: triacylglyceride, DAG: diacylglyceride, MAG: monoacylglyceride, FAEE: fatty acid ethyl ester, GLY: glycerol, EtOH: ethanol, E: enzyme, E·T, E·D, E·M: enzyme-substrate complexes, F: acyl-enzyme intermediate, I: inhibited enzyme-ethanol complex, k_i : kinetic rate constants.

The reaction rates, v , of the respective components are given as:

$$v_{\text{TAG}} = -k_1 x_E x_{\text{TAG}} + k_{-1} x_{\text{ET}} \quad (8)$$

$$v_{\text{DAG}} = k_2 x_{\text{ET}} - k_3 x_E x_{\text{DAG}} + k_{-3} x_{\text{ED}} \quad (9)$$

$$v_{\text{MAG}} = k_4 x_{\text{ED}} - k_5 x_E x_{\text{MAG}} + k_{-5} x_{\text{EM}} \quad (10)$$

$$v_{\text{FAEE}} = k_7 x_F - k_8 x_E x_{\text{EtOH}} + k_{-8} x_I \quad (11)$$

where x_i are the molar fractions of the respective species present in the system.

Assuming a pseudo-steady state for the respective concentrations of the enzyme complexes gives the following expressions:

$$\frac{dx_{\text{ET}}}{dt} = 0 = k_1 x_E x_{\text{TAG}} - k_{-1} x_{\text{ET}} - k_2 x_{\text{ET}} \quad (12)$$

$$\frac{dx_{\text{ED}}}{dt} = 0 = k_3 x_E x_{\text{DAG}} - k_{-3} x_{\text{ED}} - k_4 x_{\text{ED}} \quad (13)$$

$$\frac{dx_{\text{EM}}}{dt} = 0 = k_5 x_E x_{\text{MAG}} - k_{-5} x_{\text{EM}} - k_6 x_{\text{EM}} \quad (14)$$

$$\frac{dx_F}{dt} = 0 = k_2 x_{\text{ET}} + k_4 x_{\text{ED}} + k_6 x_{\text{EM}} - k_7 x_F \quad (15)$$

$$\frac{dx_I}{dt} = 0 = k_8 x_E x_{\text{EtOH}} - k_{-8} x_I \quad (16)$$

The total enzyme concentration of the free enzyme and the acyl-enzyme complex obeys the expression:

$$x_{\text{E,tot}} = x_E + x_{\text{ET}} + x_{\text{ED}} + x_{\text{EM}} + x_F + x_I \quad (17)$$

Rearranging Eqs. 10-15 and substituting them into Eqs. 6-9 yields:

$$v_{\text{TAG}} = \frac{-K_1 x_{\text{TAG}} x_{\text{E,tot}}}{1 + K_1 K_4 x_{\text{TAG}} + K_2 K_5 x_{\text{DAG}} + K_3 K_6 x_{\text{MAG}} + (x_{\text{EtOH}}/K_I)} \quad (18)$$

$$v_{\text{DAG}} = \frac{(K_1 x_{\text{TAG}} - K_2 x_{\text{DAG}}) x_{\text{E,tot}}}{1 + K_1 K_4 x_{\text{TAG}} + K_2 K_5 x_{\text{DAG}} + K_3 K_6 x_{\text{MAG}} + (x_{\text{EtOH}}/K_I)} \quad (19)$$

$$v_{\text{MAG}} = \frac{(K_2 x_{\text{DAG}} - K_3 x_{\text{MAG}}) x_{\text{E,tot}}}{1 + K_1 K_4 x_{\text{TAG}} + K_2 K_5 x_{\text{DAG}} + K_3 K_6 x_{\text{MAG}} + (x_{\text{EtOH}}/K_1)} \quad (20)$$

$$v_{\text{FAEE}} = \frac{(K_1 x_{\text{TAG}} + K_2 x_{\text{DAG}} + K_3 x_{\text{MAG}}) x_{\text{E,tot}}}{1 + K_1 K_4 x_{\text{TAG}} + K_2 K_5 x_{\text{DAG}} + K_3 K_6 x_{\text{MAG}} + (x_{\text{EtOH}}/K_1)} \quad (21)$$

The constants K_i in Eqs. 16-19 are:

$$K_1 = \frac{k_1 k_2}{k_{-1} + k_2} \quad (22)$$

$$K_2 = \frac{k_3 k_4}{k_{-3} + k_4} \quad (23)$$

$$K_3 = \frac{k_5 k_6}{k_{-5} + k_6} \quad (24)$$

$$K_4 = \frac{k_2 + k_7}{k_2 k_7} \quad (25)$$

$$K_5 = \frac{k_4 + k_7}{k_4 k_7} \quad (26)$$

$$K_6 = \frac{k_6 + k_7}{k_6 k_7} \quad (27)$$

$$K_1 = \frac{k_8}{k_{-8}} \quad (28)$$

According to Cheirsilp et al. [35], K_{1-3} represent the rate constants for ethanolsis of TAG, DAG, and MAG, respectively, and k_7 is the rate constant for esterification of fatty acid ethyl ester.

$$K_1 = v_{\text{mT}} \quad (29)$$

$$K_2 = v_{\text{mD}} \quad (30)$$

$$K_3 = v_{\text{mM}} \quad (31)$$

$$k_7 = v_{\text{mP}} \quad (32)$$

Similarly, the equilibrium constants for each step can be calculated as follows:

$$K_{mT} = \frac{k_1}{k_{-1} + k_2} \quad (33)$$

$$K_{mD} = \frac{k_3}{k_{-3} + k_4} \quad (34)$$

$$K_{mM} = \frac{k_5}{k_{-5} + k_6} \quad (35)$$

In this model, there are 12 unknown constants that have been estimated by fitting the model equations to the experimental data. The differential equations were solved numerically with a fourth-order Runge-Kutta method. The best fitted values were determined by minimizing the following objective function (O.F.):

$$\text{O.F.} = \frac{\sum_{\text{all samples}} \sum_{i=1}^n (x_i^{\text{exp}} - x_i^{\text{calc}})^2}{n \text{ samples}} \quad (36)$$

by using the Simplex-Nelder-Mead method. The subscript i refers to the different components in the ethanolysis system. The upperscripts “exp” and “calc” refer to the experimental and calculated molar concentrations of the different components for each experimental kinetic data (n samples).

3. Results and discussion

3.1. Ethanolysis of fish oil in SC-CO₂

Results obtained in the ethanolysis reactions at different conditions are summarized in Fig. 3. From this figure, it can be seen that production of ethyl esters (FAEE) is very rapid at the beginning of the reaction for all the tested conditions. Once most of the fish oil triacylglycerides have been consumed, the reaction becomes slower, reaching a plateau at the equilibrium conversion.

The reaction kinetics observed in this work are similar to the results obtained in previous studies [24]. The main difference from these previous studies is that SC-CO₂ reaction media considerably

enhances the reaction rates, since both the maximum FAEE production, the total TAG consumption, and the maximum MAG accumulation occur earlier in SC-CO₂, usually after 60-90 min from the beginning of the reaction, while the maximum MAG production according to Bucio et al. [31] takes place after 100 min at MR = 76:1, 303 K, 10 %wt. lipase, and 30 %wt. of *tert*-pentanol. This enhancement of the reaction performance is probably due to more favourable mass transport properties in SC-CO₂. In addition, the incorporation of SC-CO₂ as reaction media presents several advantages associated to its previously discussed green nature [15,16].

Comparing the experimental results for the ethanolysis of fish oil in SC-CO₂ catalysed by Lipozyme 435 to previous works with Lipozyme RM IM [14], higher reaction rates can be observed when using Lipozyme 435 as biocatalyst. In any case, it must be pointed out that higher catalyst loading (10 % wt.) was used in this work, which may be also responsible for the higher reaction rates, although a similar trend was also noted by Oliveira and Oliveira [21] in the ethanolysis of palm kernel oil. These authors found the homologous Novozym 435 from *C. antarctica* to attain much higher conversions in SC-CO₂ than Lipozyme IM from *Rhizomucor miehei* [21]. Other authors have also reported lipase from *C. antarctica* (Lipozyme 435 or Novozym 435) as more active and stable than Lipozyme RM IM for a wide variety of biotransformations either in supercritical, conventional, or solvent-free media [36,37].

As it can be seen when comparing the kinetics of exps. 1 and 2 (Fig. 3), initial phase behavior exert an important effect, especially on the reaction rate. According to previous studies [28], the initial loading in exp. 1 corresponds to a biphasic vapour-liquid system, thus reaction takes place in an expanded liquid, which possibly affects the actual concentrations of substrates and biocatalyst and may influence the reaction rate, as already observed before [20]. However, and according to the phase equilibria of the initial reaction system [28], we have considered the amount of reactants in the upper phase to be negligible, thus assuming an overall composition equal to the composition of the

liquid phase. On the other hand, the substrates-CO₂ ratio of exp. 2 was tuned in order to start the ethanolysis reaction in a homogeneous system. This way, mass transport limitations can be reduced and the reaction rate is enhanced, reaching total conversion of fish oil into ethyl esters (and glycerol) after 180 min from the beginning of the reaction. Additionally, from the kinetics of exp. 1, it is confirmed that Lipozyme 435 does not behave as sn-1,3-specific at low alcohol concentrations (MR = 6:1), with low MAG accumulation (0.05-0.1 mol/mol) and a significant production of GLY from the beginning of the reaction. Exp. 2 shows a slight accumulation of MAG that could indicate some specificity of the enzyme at these conditions. If we observe the initial loading (Table 1), ethanol concentration in exp. 2 is slightly higher than in exp. 1, which may have enhanced the selectivity of the biocatalyst towards MAG. Furthermore, exps. 3-6, which were carried out at a much higher ethanol concentration (MR = 76:1), corroborate the findings of Irimescu et al. [29], showing that this biocatalyst can behave as sn-1,3-specific when high concentrations of alcohol are present in the reaction media. In these conditions, we can observe MAG accumulations around 0.15-0.20 mol/mol in the initial stages of the reaction. The highest MAG production was observed at MR = 76:1, p = 10 MPa and T = 323 K (exp. 3) after 90 min of reaction, with 0.241 moles of MAG / total moles in the reaction system (ethanol-free and CO₂-free basis).

Exps. 3-6, performed at MR = 76:1 and different pressure and temperature conditions (10-30 MPa and 323-343 K, respectively) show that, at a constant pressure, increasing temperature from 323 K to 343 K slightly enhances the reaction rate. Apart from this typical Arrhenius effect [14], operating temperature may also have indirect effects, regulating the activity, specificity and stability of enzymes due to changes in the density-dependent properties of SC-CO₂ (e.g. partition coefficient, dielectric constant, Hildebrand solubility parameters) [38,39].

Comparing exps. 3 and 4 we can see the main effect of increasing temperature from 323 K to 343 K at low pressure (10 MPa), which is the lower selectivity of the reaction to MAG, since lower

accumulation of these compounds is observed at 343 K. It is also important to note that varying temperature from 323 K to 343 K at 10 MPa may have a dual effect. On the one hand, temperature enhances the reaction rate following an Arrhenius-type dependency [14]. This may explain the lower selectivity at 343 K, simply because intermediate reactions take place too fast for DAG and MAG to accumulate. On the other hand, and according to [28], the reaction at 343 K and 10 MPa initially takes place in an expanded liquid, thus stronger mass transport limitations may appear and may have contraposed to the enhancement of the reaction rate with temperature.

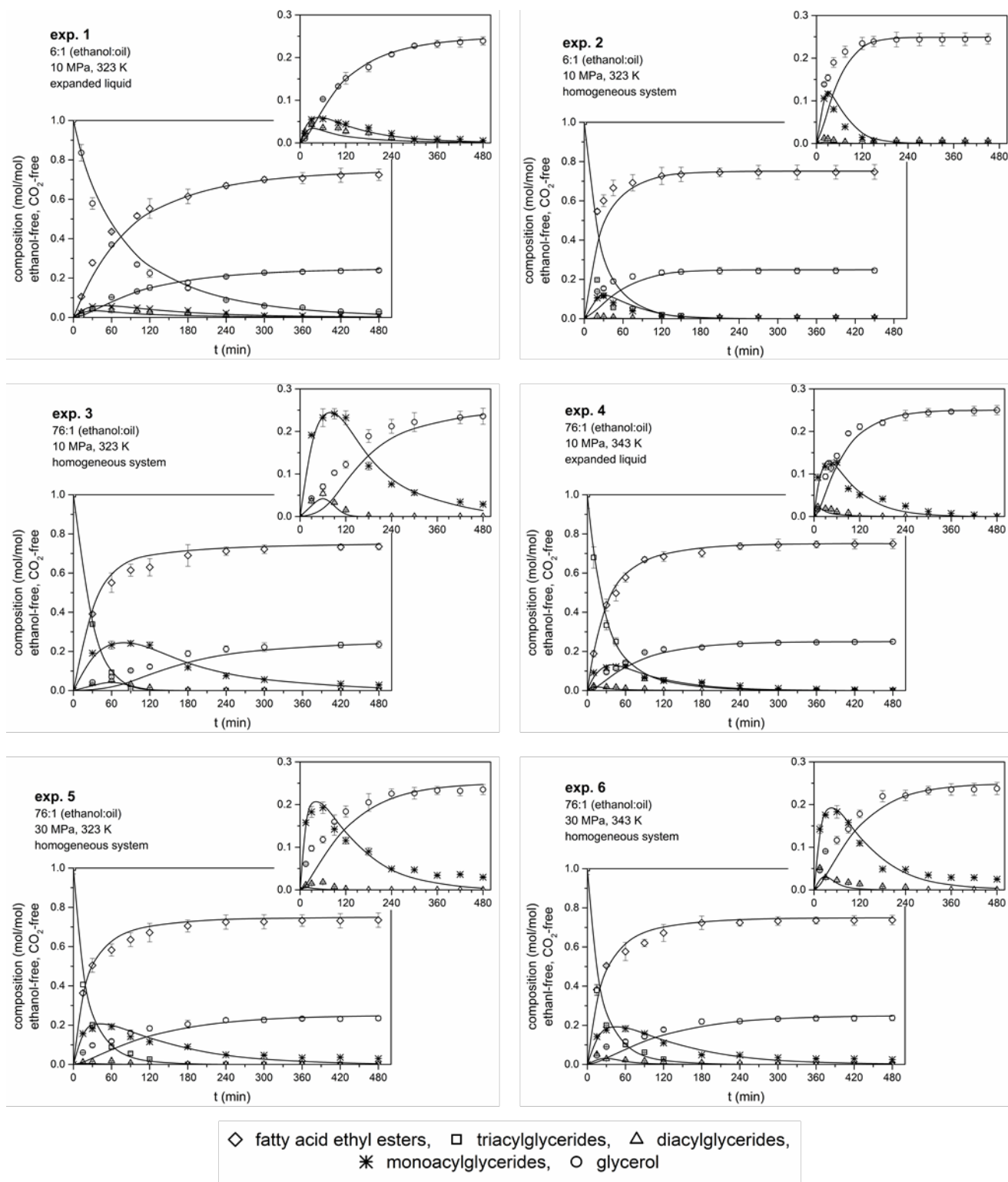


Figure 3. Time course of the ethanolysis of fish oil by Lipozyme 435 in SC-CO₂ at different reaction conditions. Enzyme loading: 10 % wt. of substrates. Lines represent the fitting of the proposed kinetic model to the experimental data.

Insert: Detail of minor components.

If we look at the effect of temperature on the reactions performed at 30 MPa (exps. 5 and 6), almost no differences can be observed except for a slightly lower MAG accumulation at 343 K. It seems that

the effect of temperature on the reaction kinetics and enzyme selectivity at 30 MPa is not as severe as it is at lower pressures. Besides, the reaction system is homogeneous at these conditions [28]; therefore, mass transport limitations due to the initial phase equilibria of the system are not expected when increasing temperature from 323 K to 343 K at 30 MPa.

As it can be seen when comparing the reactions carried out at 10 MPa (exps. 3 and 4) to those at 30 MPa (exps. 5 and 6), increasing pressure leads to faster FAEE production and earlier, although not higher, maximum of MAG. This positive effect of pressure on the reaction rate has been observed in previous works with other catalysts [14] and has been also reported for Lipozyme 435 [21]. It is generally accepted that apart from the pressure-induced conformational changes in enzymes, which may take place at much higher pressures, pressure affects enzymatic reactions in two indirect ways: (1) kinetic constants change with pressure according to transition state theory and standard thermodynamics [40], and (2) reaction rates may change with the density of SCFs because physical parameters, such as the dielectric constant, change with density [41].

In Fig. 3, the continuous lines are from the fitting of the kinetic model. As one can see, the Ping Pong Bi Bi proposed model successfully explains the experimental results. The fitted values for the kinetic constants, as well as the error made in the modeling, are summarized in Table 2.

The rate constant for the esterification of fatty acid ethyl esters step, v_{mFAEE} (k_7) is almost the same in all the experiments, thus it seems that this kinetic parameter is not affected by operating conditions. The values of v_{mFAEE} are also the highest kinetic constants among all the fitted parameters, which indicates that the production of fatty acid ethyl esters is the predominant reaction. It is also noticeable that the reaction rates of the second transesterification step, v_{mDAG} , are generally high (Table 2). Since v_{mDAG} is a rate of disappearance, these high values explain the low accumulation of DAG observed in all the experiments. In the third transesterification step, it can be observed that the

higher the MAG accumulation, the lower are the fitted values for K_{mMAG} and, especially, v_{mMAG} . Although this trend does not apply to the kinetics performed at low ethanol excess (exps. 1 and 2 with MR = 6:1), the low v_{mMAG} and K_{mMAG} can be cautiously taken as an indication of the 1,3-specificity of the biocatalyst.

Looking at the effect of initial MR, we can observe significant differences between the fitted parameters of the kinetics performed at 6:1 and those obtained for the 76:1 loading. First, v_{mTAG} and K_{mTAG} in exps. 1 and 2 (MR = 6:1) are much lower compared to the values obtained in the 76:1 kinetics. This feature can be related to the low reaction rate observed at MR = 6:1, whereas the kinetics at MR = 76:1 are generally more rapid. Besides, v_{mTAG} and K_{mTAG} in exp. 2 are slightly higher than in exp. 1, possibly reflecting the effect of the initial phase equilibria conditions. As we have previously mentioned, a monophasic reaction system like in exp. 2 would reduce mass transport limitations and accelerate the reaction kinetics, which is reflected in the higher values obtained for these kinetic parameters.

From Table 2, it can be also noticed that the rates of disappearance of DAG (v_{mDAG}) are higher in exps. 1 and 2 compared to exps. 3-6, whereas equilibrium constants (K_{mDAG}) are more similar. This may reflect the lower accumulation of DAG at MR = 6:1. Additionally, in the reactions performed at MR = 76:1, the higher v_{mDAG} , the lower the accumulation of DAG observed in the experimental results. Looking at the third reaction step, we can see that v_{mMAG} in exps. 1 and 2 are lower than in exps. 3-6, which can be explained by taking into account the low concentrations of MAG present in the reaction system at MR = 6:1. However, K_{mMAG} at MR = 6:1 are lower, which might also indicate the non-specific behaviour of the lipase at low ethanol concentrations.

The effect of changing pressure and temperature at a constant MR can be also noticed in Table 2 (exps. 3-6). The reaction rate and equilibrium constants for the first transesterification step (v_{mTAG}

and K_{mTAG}) are similar for the reactions performed at 323 K (exps. 3 and 5) and of the same order for the 343 K kinetics (exps. 4 and 6). Therefore, the effect of pressure in this reaction step is not important.

For the second and third transesterification steps, the fitted parameters (v_{mDAG} and K_{mDAG} , as well as v_{mMAG} and K_{mMAG}) are of the same order in all the experiments at MR = 76:1. Although it is true that the temperature change is more noticeable in the reactions performed at 10 MPa (exps. 3 and 4), since raising temperature increases the values of the fitted kinetic constants. This trend is a reflect of the lower accumulation of DAG and MAG that is experimentally observed in exp. 4 compared to exp. 3. On the other hand, and as we have previously discussed, the effect of temperature on the reactions performed at 30 MPa (exps. 5 and 6) is less severe. This also translates to the proposed kinetic model, in the form of almost no changes in the values of the fitted parameters.

Regarding the fitted values for the inhibition constant, K_I , Table 2 shows that the higher K_I values have been obtained in the reactions with lower ethanol excess (exps. 1 and 2, MR = 6:1). This is highly unexpected since a high ethanol concentration is supposed to displace the $E \leftrightarrow I$ equilibrium to the right-hand side, and thus a high K_I should be obtained in exps. 3-6 performed at MR = 76:1. From Table 2 is also noticeable that runs 4 and 6, performed at higher temperature (343 K) presented intermediate K_I values, closer to those of runs 1-2. A possible explanation to the values found for K_I is that this inhibition constant not only reflects the inhibitory effect of a high concentration of ethanol, but also gathers other phenomena such as mass transport limitations in the case of runs 1 and 4, and thermal inactivation of the enzyme in runs 4 and 6. The latter is especially detectable when comparing exps. 3 to 4 and 5 to 6, in which increasing the reaction temperature from 323 K to 343 K increases K_I almost 4-fold.

Table 2. Values of the kinetic rate constants (k_i), maximum reaction rates (v_{mi}), equilibrium and inhibition constants (K_{mi} and K_I) obtained in the fitting of the experimental data to the proposed Ping Pong Bi Bi kinetic model for the ethanolysis of fish oil by Lipozyme 435 in SC-CO₂ at different reaction conditions. The objective function (O.F.) indicates the error made in the fitting.

run	k_1 (min ⁻¹)	k_{-1} (min ⁻¹)	k_2 (min ⁻¹)	v_{mTAG}^* (min ⁻¹)	K_{mTAG}^* (mmol ¹)	k_3 (min ⁻¹)	k_{-3} (min ⁻¹)	k_4 (min ⁻¹)	v_{mDAG}^* (min ⁻¹)	K_{mDAG}^* (mmol ¹)	k_5 (min ⁻¹)	k_{-5} (min ⁻¹)	k_6 (min ⁻¹)	v_{mMAG}^* (min ⁻¹)	K_{mMAG}^* (mmol ¹)	$k_7 =$ v_{mFAEE} (min ⁻¹)	K_I^*	O.F.*
1	1.491	61.76	9.383	0.197	0.021	103.3	12.47	65.87	86.86	1.319	6.280	44.41	12.68	1.395	0.110	180.3	1.441	0.0923
2	5.549	61.67	9.984	0.773	0.077	103.3	12.49	65.87	86.84	1.318	6.390	44.40	12.74	1.425	0.112	180.3	1.447	0.0666
3	36.65	51.33	32.03	14.08	0.440	81.66	35.43	28.20	36.19	1.283	9.685	32.33	10.55	2.383	0.226	179.8	0.383	0.0037
4	9.326	55.93	18.04	2.275	0.126	93.09	14.83	37.51	66.71	1.778	11.91	29.86	12.32	3.477	0.282	179.7	1.264	0.0004
5	35.62	54.02	35.91	14.23	0.396	95.43	32.83	37.93	51.15	1.349	10.42	29.88	11.69	2.928	0.251	179.6	0.302	0.0009
6	16.77	55.48	21.76	4.725	0.217	91.05	19.60	36.29	59.12	1.629	11.83	29.81	10.04	2.981	0.297	179.8	0.923	0.0011

*see Eqs. (28-36).

3.2. Purification of reaction products

Reaction conditions of exp. 3 (MR = 76:1, 323 K, and 10 MPa) were selected as the optimal for further purification of reaction products by SFE since maximum MAG accumulation was observed at $t = 90$ min (MAG molar fraction = 0.241). However, reaction products were collected at 120 min in order to reduce TAG and DAG as much as possible. In order to avoid an entrainer effect of ethanol, its content was reduced by means of vacuum-evaporation, obtaining an initial feed with the following composition: 58.2 % FAEE, 38.4 % MAG, 1.3 % EtOH, 0.002 % TAG, 1.7 % DAG, and 0.4 % GLY (% wt.). In a possible industrial process, ethanol removal can be performed in a pre-fractionation step with a continuous countercurrent packed column, using SC-CO₂ as the separation agent.

A total of 10 SFE runs were performed with this mixture as initial feed, varying pressure and temperature at a constant CO₂ mass flow of 1.8 ± 0.2 g/min. Results are summarized in Table 3, where it can be seen that the most volatile compounds (EtOH, FAEE, and low amounts of MAG) were preferentially collected in the extract, while GLY, DAG, and especially MAG remained in the extractor since they are less soluble in liquid or SC-CO₂ [42], thus the raffinate was concentrated in these compounds. Traces of TAG (< 0.01 % wt.) were also detected in the raffinate (Table 3).

Calculated *K*-ratios for FAEE reflect the selective extraction of FAEE, since they are greater than unity in all SFE runs. At the same time, the *K*-ratios for MAG are much lower than unity, indicating that MAG were concentrated in the raffinate up to 82.25 % wt. in run 4 (Table 3). Nevertheless, total MAG purification was not achieved in the experimental range studied. On the contrary, nearly pure (99.5 % wt.) FAEEs were extracted in run 7 at 11.5 MPa and 333 K, although the extract yield in this run was very low. SC-CO₂ at low pressure and moderate temperature is not able to solubilize and extract the less soluble acylglycerides (DAG and MAG) [42], resulting in high selectivities to FAEE although low yields. An alternative to increase the yield without affecting the selectivity might be to increase the solvent-to-feed ratio with a higher CO₂ mass flow and/or longer extraction times,

although the feasibility of this process at larger scale should be determined through economic analysis.

Table 3. Summary of results obtained in the supercritical fluid extraction experiments. Extract (E) and Raffinate (R) yields (ϵ), Composition (%wt.), and partition ratios (K -ratios) of the components of the reaction mixture (fatty acid ethyl esters, FAEE; monoacylglycerides, MAG; ethanol, EtOH; triacylglycerides, TAG; diacylglycerides, DAG; and glycerol, GLY).

run	exp. conditions		composition (%wt.)																
			ϵ^* (%)		feed	FAEE			MAG			EtOH		TAG		DAG		GLY	
	P (MPa)	T (K)	E	R		E	R	K -ratio [†]	E	R	K -ratio [†]	E	R	E	R	E	R	E	R
						58.2				38.4			1.3		0.002		1.7		0.4
1	10	313	17.5	79.4		95.0	50.4	1.88	2.9	46.0	0.01	2.1	1.1	n.d.	0.002	n.d.	2.0	n.d.	0.5
2	15	313	28.3	67.4		94.4	43.9	2.15	3.6	52.2	0.07	2.0	1.0	n.d.	0.003	n.d.	2.3	n.d.	0.6
3	20	313	54.4	39.1		94.1	15.5	6.09	4.3	79.1	0.05	1.6	0.9	n.d.	0.004	n.d.	3.6	n.d.	0.9
4	28	313	67.0	27.7		81.6	10.7	7.61	16.8	82.3	0.20	1.6	0.7	n.d.	0.006	n.d.	5.0	n.d.	1.3
5	10	298	29.4	64.9		94.1	43.2	2.18	4.4	52.6	0.08	1.4	1.2	n.d.	0.003	n.d.	2.4	n.d.	0.6
6	20	298	49.1	48.3		92.1	25.6	3.60	6.6	69.1	0.10	1.4	1.2	n.d.	0.004	n.d.	3.3	n.d.	0.8
7	11	333	5.5	93.3		99.5	55.8	1.78	0.0	40.7	0.00	0.5	1.3	n.d.	0.002	n.d.	1.8	n.d.	0.4
8	15	333	16.1	78.0		96.7	50.8	1.90	3.2	45.2	0.07	0.1	1.5	n.d.	0.002	n.d.	2.0	n.d.	0.5
9	20	333	32.3	66.6		82.6	46.6	1.77	15.3	49.5	0.31	2.1	0.9	n.d.	0.003	n.d.	2.5	n.d.	0.6
10	28	333	42.0	53.0		80.5	42.1	1.91	17.2	53.8	0.32	2.4	0.5	n.d.	0.003	n.d.	2.9	n.d.	0.7

Standard uncertainties: $u(p) = \pm 0.5$ MPa, $u(T) = \pm 0.1$ K, $u(w_i) = \pm 0.5$ %.

* $\epsilon_{\text{extract}} (\%) = \text{extract}/\text{feed} \cdot 100$; $\epsilon_{\text{raffinate}} (\%) = \text{raffinate}/\text{feed} \cdot 100$

† $K\text{-ratio}_i = i_{\text{extract}}/i_{\text{raffinate}}$

Fig. 4 depicts the effects of CO₂ density, calculated from [43], on the purity and recovery of FAEE and MAG in the extract and raffinate, respectively, showing an opposite behavior of these parameters when varying density. In Fig. 4 (left), FAEE recovery increases with higher densities, yet FAEE purity in the extract decreases. According to literature [44], solubility of fatty acid ethyl esters in SC-CO₂ increases with pressure and temperature, which increases the recovery. However, other compounds present in the feed mixture become more soluble in CO₂, which in turn would decrease the purity of the extract.

In the raffinate, the MAG purity increases with density (Fig. 4, right) since the more volatile compounds such as FAEE and EtOH are more soluble in SC-CO₂, thus they are more easily extracted. However, solubility of the shorter-chain, more saturated MAG also increases, which slightly decreases the MAG recovery at higher densities.

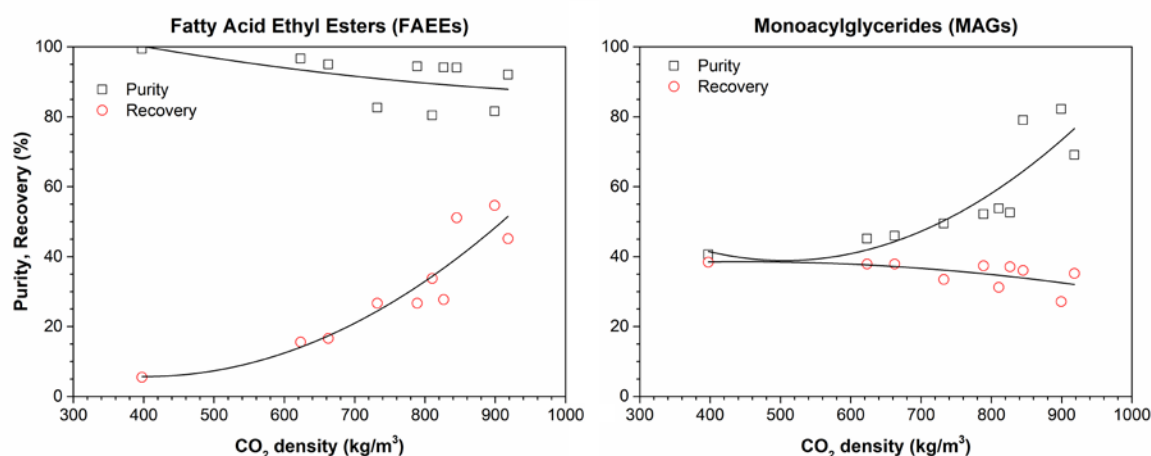


Figure 4. Effect of density of CO₂ on the purity (open squares) and recovery (open circles) of fatty acid ethyl esters in the extract and monoacylglycerides in the raffinate. CO₂ density values were calculated based on [43]. Lines are drawn to guide the eye.

This trend has been also observed by Soto et al. [19] in the simulated fractionation of a 80 %wt. FAME and 20 %wt. MAG mixture. These authors observed that higher CO₂ to feed ratios (from 7 kg CO₂/kg feed to 17 kg/kg) were necessary to refine MAG when raising temperature from 298 K to 313 K at constant pressure (~11 MPa) (i.e.: decreasing density). Results obtained in this work are

also comparable to those obtained by Compton et al. [18] in the purification of 2-MAG obtained from ethanolysis of TAG using liquid CO₂ (298 K, 8.62 MPa). Maximum MAG purity in this work was also ~80%, although it was obtained at supercritical conditions (313 K, 20 MPa) and some FAEE residues remained in the raffinate.

Fatty acid profile of the initial feed, extract and raffinate were also analyzed by GC. Results are shown in Fig. 5, where it can be seen that saturated fatty acids (SFAs) accumulated in the extract while polyunsaturated fatty acids (PUFAs), and especially those from the omega-3 series EPA and DHA, remained in the raffinate. These results were expected since SFAs are more soluble in SC-CO₂ than the longer-chain, less saturated PUFAs [42], so the former would be preferentially solubilized and extracted by SC-CO₂. Besides, fish oil SFAs are mostly located in the sn-1(3) position of the triacylglyceride [7], thus most of them would have been transformed to the more soluble FAEE form in the previous ethanolysis step. On the other hand, SC-CO₂ was not selective to monounsaturated fatty acids, MUFA, as we can find similar concentrations both in the extract and the raffinate (Fig. 5).

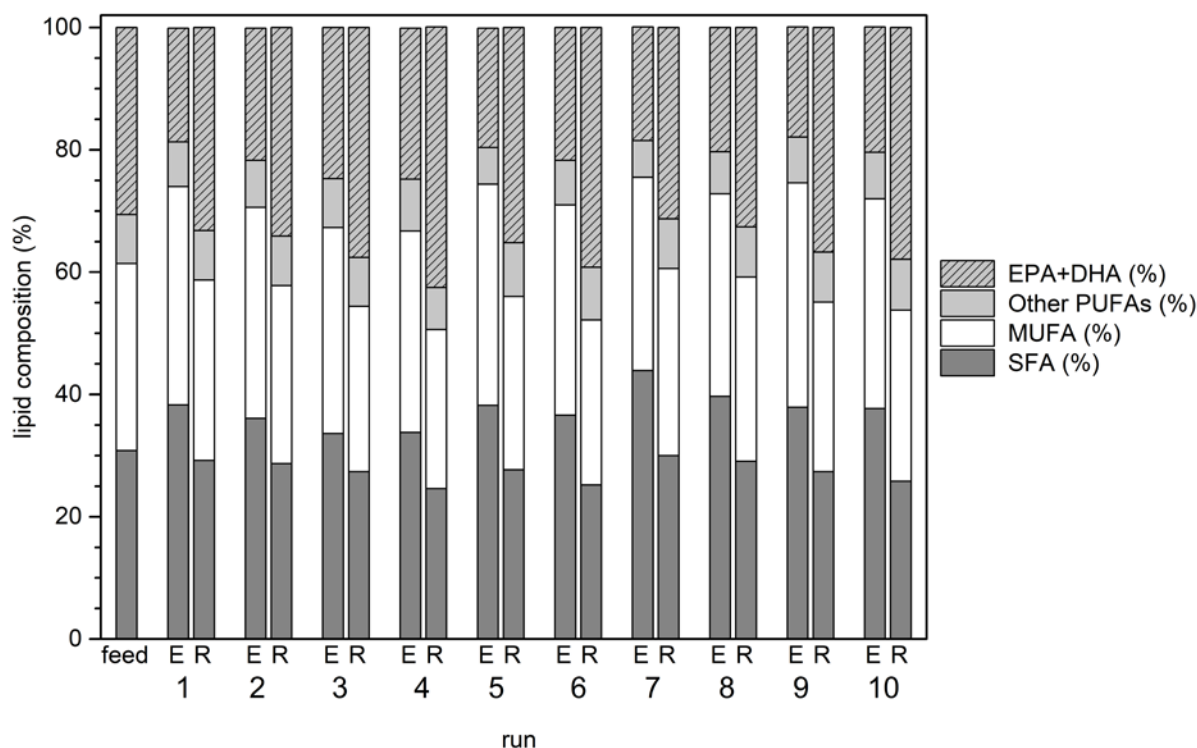


Figure 5. Fatty acid distribution of the initial feed, extract (E) and raffinate (R), obtained in the SFE experiments.

Taking these results into account, it is evident that a compromise between purity and recovery should be made, and both for FAEE and MAG. Experimental conditions in SFE run 3 (20.5 MPa, 313 K) allowed a FAEE recovery of 51.2 % with 94.1 % purity, and at the same time a MAG recovery of 36.1 % with 79.1 % purity. EPA+DHA content in the raffinate was 37.6 % wt., which represents an enrichment of 18 % compared to the initial fish oil.

Conclusions

Supercritical carbon dioxide (SC-CO₂) has been used as a green solvent in the ethanolysis of fish oil by Lipozyme 435. Triacylglycerides have been specifically transformed into monoacylglycerides and fatty acid ethyl esters at high ethanol-to-oil molar ratios. Lipozyme 435-catalyzed ethanolysis in SC-CO₂ appears as a suitable method to obtain monoacylglycerides and fatty acid ethyl esters with higher reaction rates compared to other biocatalysts and reaction media.

Operating pressure and temperature affect the reaction performance and its specificity through changes in the reaction rate, the density-dependent physical parameters of the solvent, and the phase behaviour of the reaction system. Correlation of experimental data to a kinetic model based on the Ping Pong Bi Bi mechanism showed that the rate constant for esterification of fatty acid ethyl ester is not affected by experimental conditions. The same is not true for the ethanolysis steps, which change with the initial molar ratio, pressure and temperature, and therefore determine the reaction performance and selectivity.

Purification of fish oil ethanolysis reaction products by supercritical fluid extraction is a suitable technique to concentrate fatty acid ethyl esters in the extract and monoacylglycerides in the raffinate. SC-CO₂ also discriminates between saturated and polyunsaturated fatty acids. These promising results can be taken as a basis for the development of a continuous, industrially-feasible supercritical

fractionation process for the production of omega-3 PUFAs in the natural, more bioavailable monoacylglyceride form.

Acknowledgments

To the Spanish Government through MINECO and the European Regional Development Fund (ERDF) for financial support [grant number CTQ2012-39131-C02-01] and RM's and AEI's contracts [BES-2013-063937, CTQ2015-64396-R]. To Junta de Castilla y León and ERDF for financial support [grant number BU055U16] and ÓBR's post-doctoral contract.

References

- [1] A.P. Simopoulos, Omega-3 fatty acids in health and disease and in growth and development, *Am. J. Clin. Nutr.* 54 (1991) 438–463. doi:10.1093/ajcn/54.3.438.
- [2] P.M. Kris-Etherton, W.S. Harris, L.J. Appel, Fish consumption, fish oil, omega-3 fatty acids, and cardiovascular disease, *Circulation.* 106 (2002) 2747–2757. doi:10.1161/01.CIR.0000038493.65177.94.
- [3] P.C. Calder, Mechanisms of action of (n-3) fatty acids, *J. Nutr.* 142 (2012) 592S–599S. doi:10.3945/jn.111.155259.
- [4] S. Kalmijn, L.J. Launer, A. Ott, J.C.M. Witteman, A. Hofman, M.M.B. Breteler, Dietary fat intake and the risk of incident dementia in the Rotterdam study, *Ann. Neurol.* 42 (1997) 776–782. doi:10.1002/ana.410420514.
- [5] M.C. Morris, D.A. Evans, J.L. Bienias, C.C. Tangney, D.A. Bennett, R.S. Wilson, N. Aggarwal, J. Schneider, Consumption of fish and n-3 fatty acids and risk of incident Alzheimer disease, *Arch. Neurol.* 60 (2003) 940–946. doi:10.1001/archneur.60.7.940.
- [6] F. Calon, G.P. Lim, F. Yang, T. Morihara, B. Teter, O. Ubeda, P. Rostaing, A. Triller, N. Salem Jr., K.H. Ashe, S.A. Frautschy, G.M. Cole, Docosahexaenoic acid protects from dendritic pathology in an Alzheimer's disease mouse model, *Neuron.* 43 (2004) 633–645. doi:10.1016/j.neuron.2004.08.013.
- [7] Á.G. Solaesa, S.L. Bucio, M.T. Sanz, S. Beltrán, S. Rebolleda, Characterization of triacylglycerol composition of fish oils by using chromatographic techniques, *J. Oleo Sci.* 63 (2014) 449–460. doi:10.5650/jos.ess13202.
- [8] R. Melgosa, Ó. Benito-Román, M.T. Sanz, E. de Paz, S. Beltrán, Omega-3 encapsulation by

- PGSS-drying and conventional drying methods. Particle characterization and oxidative stability, *Food Chem.* 270 (2019) 138–148. doi:10.1016/j.foodchem.2018.07.082.
- [9] M.M.C. Feltes, P. Villeneuve, B. Baréa, N. Barouh, J.V. de Oliveira, D. de Oliveira, J.L. Ninow, Enzymatic production of monoacylglycerols (MAG) and diacylglycerols (DAG) from fish oil in a solvent-free system, *J. Am. Oil Chem. Soc.* 89 (2012) 1057–1065. doi:10.1007/s11746-011-1998-2.
- [10] C. Cruz-Hernandez, S.K. Thakkar, J. Moulin, M. Oliveira, I. Masserey-Elmelegy, F. Dionisi, F. Destaillets, Benefits of structured and free monoacylglycerols to deliver eicosapentaenoic (EPA) in a model of lipid malabsorption, *Nutrients.* 4 (2012) 1781–1793. doi:10.3390/nu4111781.
- [11] F. Shahidi, U.N. Wanasundara, Omega-3 fatty acid concentrates: Nutritional aspects and production technologies, *Trends Food Sci. Technol.* 9 (1998) 230–240. doi:10.1016/S0924-2244(98)00044-2.
- [12] N. Rubio-Rodríguez, S. Beltrán, I. Jaime, S.M. de Diego, M.T. Sanz, J.R. Carballido, Production of omega-3 polyunsaturated fatty acid concentrates: a review, *Innov. Food Sci. Emerg. Technol.* 11 (2010) 1–12. doi:10.1016/j.ifset.2009.10.006.
- [13] R. Melgosa, M.T. Sanz, Á.G. Solaesa, S.L. Bucio, S. Beltrán, Enzymatic activity and conformational and morphological studies of four commercial lipases treated with supercritical carbon dioxide, *J. Supercrit. Fluids.* 97 (2015) 51–62. doi:10.1016/j.supflu.2014.11.003.
- [14] R. Melgosa, M.T. Sanz, Á.G. Solaesa, E. de Paz, S. Beltrán, D.L. Lamas, Supercritical carbon dioxide as solvent in the lipase-catalyzed ethanolysis of fish oil: Kinetic study, *J. CO₂ Util.* 17 (2017) 170–179. doi:10.1016/j.jcou.2016.11.011.
- [15] E. Jenab, F. Temelli, J.M. Curtis, Y.Y. Zhao, Performance of two immobilized lipases for interesterification between canola oil and fully-hydrogenated canola oil under supercritical carbon dioxide, *LWT - Food Sci. Technol.* (2014). doi:10.1016/j.lwt.2014.02.051.
- [16] Ž. Knez, Enzymatic reactions in dense gases, *J. Supercrit. Fluids.* 47 (2009) 357–372. doi:10.1016/j.supflu.2008.11.012.
- [17] T. Matsuda, Recent progress in biocatalysis using supercritical carbon dioxide., *J. Biosci. Bioeng.* 115 (2013) 233–41. doi:10.1016/j.jbiosc.2012.10.002.
- [18] D.L. Compton, F.J. Eller, J.A. Laszlo, K.O. Evans, Purification of 2-monoacylglycerols using liquid CO₂ extraction, *JAOCs, J. Am. Oil Chem. Soc.* 89 (2012) 1529–1536. doi:10.1007/s11746-012-2035-9.
- [19] G. Soto, P. Hegel, S. Pereda, Supercritical production and fractionation of fatty acid esters and acylglycerols, *J. Supercrit. Fluids.* 93 (2014) 74–81. doi:10.1016/j.supflu.2014.04.017.
- [20] H. Gunnlaugsdottir, B. Sivik, Lipase-catalyzed alcoholysis of cod liver oil in supercritical carbon dioxide, *J. Am. Oil Chem. Soc.* 72 (1995) 399–405. doi:10.1007/BF02636078.
- [21] J.V. Oliveira, D. Oliveira, Kinetics of the enzymatic alcoholysis of palm kernel oil in supercritical CO₂, *Ind. Eng. Chem. Res.* 39 (2000) 4450–4454. doi:10.1021/ie990865p.
- [22] D. Oliveira, J.V. Oliveira, Enzymatic alcoholysis of palm kernel oil in n-hexane and SCCO₂,

- J. Supercrit. Fluids. 19 (2001) 141–148. doi:10.1016/S0896-8446(00)00068-1.
- [23] S.-K. Shin, J.-E. Sim, H. Kishimura, B.-S. Chun, Characteristics of menhaden oil ethanolysis by immobilized lipase in supercritical carbon dioxide, J. Ind. Eng. Chem. 18 (2012) 546–550. doi:10.1016/j.jiec.2011.11.065.
- [24] H.Y. Lee, A.S.M. Tanbirul-Haque, S.B. Kim, Y.B. Lee, B.S. Chun, Effect of reaction parameters on conversion of krill (*Euphausia superba*) oil by immobilized lipase ethanolysis, J. Ind. Eng. Chem. 20 (2014) 1097–1102. doi:10.1016/j.jiec.2013.06.047.
- [25] M. Kondo, K. Rezaei, F. Temelli, M. Goto, On-line extraction - reaction of canola oil with ethanol by immobilized lipase in SC-CO₂, Ind. Eng. Chem. Res. 41 (2002) 5770–5774. doi:10.1021/ie010816o
- [26] A. Baiker, Supercritical Fluids in Heterogeneous Catalysis, Chem. Rev. 99 (1999) 453–474. doi:10.1021/cr970090z.
- [27] E. Brignole, S. Pereda, Phase Equilibrium Engineering Principles in Reactive Systems, in: E. Brignole, S. Pereda (Eds.), Phase Eq. Eng., Elsevier, 2013: pp- 263–298. doi:10.1016/B978-0-444-56364-4.00011-X.
- [28] R. Melgosa, M.T. Sanz, Á.G. Solaesa, S. Beltrán, Phase behaviour of the pseudo-ternary system carbon dioxide + ethanol + fish oil at high pressures, J. Chem. Thermodyn. 115 (2017) 106–113. doi:10.1016/j.jct.2017.07.032.
- [29] R. Irimescu, Y. Iwasaki, C.T. Hou, Study of TAG ethanolysis to 2-MAG by immobilized *Candida antarctica* lipase and synthesis of symmetrically structured TAG, JAOCS, J. Am. Oil Chem. Soc. 79 (2002) 879–883. doi:10.1007/s11746-002-0573-8.
- [30] S.L. Bucio, A.G. Solaesa, M.T. Sanz, S. Beltrán, R. Melgosa, Liquid-liquid equilibrium for ethanolysis systems of fish oil, J. Chem. Eng. Data. 58 (2013) 3118–3124. doi:10.1021/je400573u.
- [31] S.L. Bucio, Á.G. Solaesa, M.T. Sanz, R. Melgosa, S. Beltrán, H. Sovová, Kinetic study for the ethanolysis of fish oil catalyzed by Lipozyme 435 in different reaction media, J. Oleo Sci. 64 (2015) 431–441.
- [32] Á.G. Solaesa, M.T. Sanz, M. Falkeborg, S. Beltrán, Z. Guo, Production and concentration of monoacylglycerols rich in omega-3 polyunsaturated fatty acids by enzymatic glycerolysis and molecular distillation, Food Chem. 190 (2016) 960–967. doi:10.1016/j.foodchem.2015.06.061.
- [33] Official methods of analysis of the Association of Official Analytical Chemists. AOAC Official Method 2012.13. Determination of labeled fatty acids content in milk products and infant formula, Washington, DC, 2012.
- [34] W.B. Nilsson, Supercritical Fluid Extraction and Fractionation of Fish Oil, in: J.W. King, G.R. List (Eds.), Supercrit. Fluid Technol. Oil Lipid Chem., AOCS Press, 1996: pp. 181–212. doi:10.1002/food.19970410220.
- [35] B. Cheirsilp, A. H-Kittikun, S. Limkatanyu, Impact of transesterification mechanisms on the kinetic modeling of biodiesel production by immobilized lipase, Biochem. Eng. J. 42 (2008) 261–269. doi:10.1016/j.bej.2008.07.006.

- [36] M.D. Romero, L. Calvo, C. Alba, A. Daneshfar, H.S. Ghaziaskar, Enzymatic synthesis of isoamyl acetate with immobilized *Candida antarctica* lipase in n-hexane, *Enzyme Microb. Technol.* 37 (2005) 42–48. doi:10.1016/j.enzmictec.2004.12.033.
- [37] A.B. Martins, A.M. Da Silva, M.F. Schein, C. Garcia-Galan, M.A. Záchia Ayub, R. Fernandez-Lafuente, R.C. Rodrigues, Comparison of the performance of commercial immobilized lipases in the synthesis of different flavor esters, *J. Mol. Catal. B Enzym.* 105 (2014) 18–25. doi:10.1016/j.molcatb.2014.03.021.
- [38] M. V Oliveira, S.F. Rebocho, A.S. Ribeiro, E.A. Macedo, J.M. Loureiro, Kinetic modelling of decyl acetate synthesis by immobilized lipase-catalysed transesterification of vinyl acetate with decanol in supercritical carbon dioxide, *J. Supercrit. Fluids.* 50 (2009) 138–145. doi:10.1016/j.supflu.2009.05.003.
- [39] M. Habulin, S. Šabeder, M. Paljevac, M. Primožič, Ž. Knez, Lipase-catalyzed esterification of citronellol with lauric acid in supercritical carbon dioxide/co-solvent media, *J. Supercrit. Fluids.* 43 (2007) 199–203. doi:10.1016/j.supflu.2007.05.001.
- [40] S. V Kamat, E.J. Beckman, A.J. Russell, Enzyme activity in supercritical fluids, *Crit. Rev. Biotechnol.* 15 (1995) 41–71. doi:10.3109/07388559509150531.
- [41] O. Aaltonen, Enzymatic Catalysis, in: P.G. Jessop, W. Leitner (Eds.), *Chem. Synth. Using Supercrit. Fluids*, Wiley-VCH Verlag GmbH, 1999: p. 414. doi:10.1002/9783527613687.ch19.
- [42] Ö. Güçlü-Üstundağ, F. Temelli, Correlating the solubility behavior of fatty acids, mono-, di-, and triglycerides, and fatty acid esters in supercritical carbon dioxide, *Ind. Eng. Chem. Res.* 39 (2000) 4756–4766 . doi: 10.1021/ie0001523.
- [43] R. Span, W. Wagner, A new equation of state for carbon dioxide covering the fluid region from the triple-point temperature to 1100 K at pressures up to 800 MPa, *J. Phys. Chem. Ref. Data.* 25 (1996) 1509–1596. doi: 10.1063/1.555991
- [44] V. Riha, G. Brunner, Phase equilibrium of fish oil ethyl esters with supercritical carbon dioxide, *J. Supercrit. Fluids.* 15 (1999) 33–50. doi:10.1016/S0896-8446(98)00130-2.